ELECTRONIC SUPPLEMENTARY INFORMATION

In situ structural analysis with a SAXS laboratory beamline directly in a microfluidic chip. Supplementary information.

Radajewski Dimitri,* Pierre Roblin, Patrice Bacchin, Martine Meireles, Yannick Hallez*

1 Modelling

1.1 Modelling of the form factor of a polydisperse suspension

Consider a polydisperse sphere suspension with a diameter distribution given by $d(\sigma;\bar{\sigma},\sigma')$ where $\bar{\sigma}$ is the average diameter and σ' is RMS deviation from $\bar{\sigma}$. The form factor can be computed as the weighted average

$$\bar{P}(q) = \frac{\text{factor}}{V}\int_{\sigma=0}^{\infty} d(\sigma;\bar{\sigma},\sigma')f^2(q,\sigma)d\sigma + \text{background} \qquad (1)$$

where $f(q,\sigma)$ is the scattering amplitude of a sphere of diameter σ. In the Rayleigh-Gans-Debye approximation valid here, it is given by

$$f(q,\sigma) = (\nu_p - \nu_s)\sigma^3 b(q\sigma/2), \qquad (2)$$

where ν_p and ν_s are the particle and solvent refractive indices, and $b(x) = j_1(x)/x$ is the form amplitude of the sphere, with j_1 being the spherical Bessel function of first order. Here we modelled the distribution of radii with the Schulz distribution

$$d(\sigma;\bar{\sigma},\sigma') = (t+1)^{t+1}\left(\frac{\sigma}{\overline{\sigma}}\right)^t \frac{\exp[-(t+1)\sigma/\overline{\sigma}]}{\overline{\sigma}\Gamma(t+1)}, \qquad (3)$$

where $t = 1/s^2 - 1$, $s = \sigma'/\overline{\sigma}$ is the relative polydispersity, and Γ is the Gamma function. The distribution parameters $\overline{\sigma}$ and σ' were obtained by fitting the experimental SAXS intensity at large dilution to avoid any influence of colloidal interactions. The positions of the first signal decrease and of the secondary peak allowed to fit the mean diameter. Polydispersity was adjusted to match the smoothing of the scattering data between peaks.

To model the measurable structure factor $S_M(q)$ of the polydisperse suspension, we will first need to transfer the fit of the experimental $P(q)$ by a continuous Schulz distribution to a "histogrammatic" distribution of m species identified by indices $\alpha = 1,\ldots,m$, with discrete diameters σ_α and molar fractions x_α. These $2m$ parameters can be determined by matching the first $2m$ moments of the continuous Schulz distribution to those of the histogrammatic distribution. This is possible because they are known analytically:

$$\langle\sigma^n\rangle = \frac{(n+t)!}{t!(t+1)^n}\bar{\sigma}^n = \sum_{\alpha=1}^{m} x_\alpha\sigma_\alpha^n \quad \text{for} \quad n = 0,\ldots,2m-1 \qquad (4)$$

Laboratoire de Génie Chimique, Université de Toulouse, CNRS, INPT, UPS, Toulouse, France. E-mail: dimitri.radajewski@gmail.com, yannick.hallez@univ-tlse3.fr

The number of species m can be chosen arbitrarily. It has been shown that using $m = 3$ was sufficient for relative polydispersities s lower than 0.3.[1] Here we considered systems with maximum polydispersities of about 0.15 and, indeed, using $m = 3$ or $m = 5$ led to virtually identical results.

At this point, we have modelled the particle sizes with both a continuous distribution used to plot the form factors in the main text and with a histogrammatic distribution used to compute an approximation of the measurable structure factor.

1.2 Modelling of the measurable structure factor of a multicomponent suspension

In this section, we essentially follow the lines of Reference 1. The intensity scattered by a multicomponent suspension of m species of spheres is

$$I(q) = N\overline{f^2}(q=0)\overline{P}(q)S_M(q),$$

where N is the number of scatterers,

$$\overline{f^2}(q) = \sum_{\alpha=1}^{m} x_\alpha f_\alpha^2(q) \qquad (5)$$

is the second moment of the distribution of scattering amplitudes from each component $f_\alpha(q) = f(q,\sigma_\alpha)$,

$$\overline{P}(q) = \frac{\overline{f^2}(q)}{\overline{f^2}(q=0)} \qquad (6)$$

is the average form factor, and

$$S_M(q) = \frac{1}{\overline{f^2}(q)}\sum_{\alpha,\beta=1}^{m}\sqrt{x_\alpha x_\beta}f_\alpha(q)f_\beta(q)S_{\alpha\beta}(q) \qquad (7)$$

is the measurable static structure factor, where $S_{\alpha\beta}(q)$ are the partial static structure factors.[2] After the fit of the form factor described in the previous section, m, σ_α and x_α are known, so eq. (5) and (6) are readily computed. Computing $S_M(q)$ with eq. (7) is possible in principle by first solving the multicomponent Ornstein-Zernike (OZ) equation for the $S_{\alpha\beta}(q)$ with a suitable closure but it involves rather complicated and possibly unstable codes, and more importantly, it requires defining m effective particle charges (one for each species), a task for which there is no exact analytical method. If the polydispersity is below about 0.2, the complexity of the modelling can be greatly reduced by invoking the decoupling approximation. Assuming the system is

polydisperse in size but not in charge, the measurable structure factor (7) is then

$$S_M(q) \simeq (1 - X(q))S^{id}(q) + X(q), \tag{8}$$

where

$$X(q) = 1 - \frac{\bar{f}(q)^2}{\overline{f^2}(q)}$$

and $S^{id}(q)$ is the structure factor of an "ideal" monodisperse suspension with effective diameter σ^{eff} and charge Z^{eff}. Now we only need to solve the one-component OZ equation. Parameters σ^{eff} and Z^{eff} can be modelled or fitted. Here the diameter of the ideal monodisperse suspension is defined as

$$\sigma^{eff} = \left(\sum_{\alpha=1}^{m} x_\alpha \sigma_\alpha^3 \right)^{1/3}$$

so the volume fraction of the ideal monodisperse suspension is the same as that of the polydisperse system. Note that there is no proof that this could be an ideal choice. The relation between particle size and effective particle charge Z^{eff} (accounting for polydispersity *and* ion condensation) to be used in the ideal monodisperse suspension is unknown. Here, we first considered that the true bare surface charge density σ_e carried by all the colloids was the same. It is not unreasonable as it depends mostly on surface chemistry and not too much the particle size. Then the bare surface charge carried by particles of type α is $Z_\alpha = \pi\sigma_\alpha^2\sigma_e$ and the bare charge of the ideal monodisperse system was approximated by

$$Z^{id} = \sum_{\alpha=1}^{m} x_\alpha Z_\alpha.$$

We then used the Extrapolated Point Charge renormalization procedure[3] to define a unique effective charge Z^{eff} and a renormalized inverse screening length κ^{eff} from the actual salt content and Z^{id}. Note that the choice of a constant surface charge density has been made here and in Ref.[1] but different choices of effective parameters could have been made. For example, the Z_α^{eff} could be computed from a polydisperse renormalization scheme[4,5] and Z^{eff} would then be defined in an ad hoc manner (for example with a weighted average) or Z^{eff} could also just be left as a fitting parameter as in Ref. 6. As no theory is available to define σ^{eff} and Z^{eff} unambiguously, any choice is somewhat arbitrary and has to be supported *a posteriori* by comparisons with experiments. The choices made here were suitable to model the measurable structure factors of silica and latex dispersions, but other choices would probably have been good too as the polydispersity was relatively modest.

1.3 Modelling of the ideal monodisperse structure factor

Once choices of the effective parameters σ^{eff}, Z^{eff}, and κ^{eff} were made as described above, the "ideal" structure factor involved in eq. (8) was computed by solving the one-component Ornstein-Zernike (OZ) equation for an effective interaction potential of the Hard-Sphere-Yukawa (HSY) form. Dropping the *eff* superscripts for conciseness and introducing the sphere radius $a = \sigma/2$, the HSY potential reads

$$\beta u(r) = \begin{cases} Z^2 l_B \frac{e^{2\kappa a}}{(1+\kappa a)^2} \frac{e^{-\kappa r}}{r}, & r \geq 2a \\ \infty, & r < 2a \end{cases} \tag{9}$$

where $\beta = 1/kT$ and $l_B = e^2/4\pi\varepsilon kT$ is the Bjerrum length, k is Boltzmann's constant, T is the temperature, e is the elementary charge, and ε is the permittivity of the solvent. To solve the OZ equation, the Rogers-Young[7] (RY) closure was chosen as it is known to yield accurate results for charged hard spheres.[8–11]

2 SAXS data for the latex dispersions in standard capillaries

Measurements of scattering from latex dispersions have been undertaken both in the microfluidic chip and in standard capillaries for comparison. Results can be compared in Fig. 1. The noisy signals visible at low q in the chip are absent in capillaries due to the increased signal to noise ratio. The background is also one order of magnitude smaller in capillaries, which makes the modelling easier especially at high dilution. However, the first structure peak is identical in both setups as expected, which highlights the possibility to measure colloidal interactions.

Notes and references

1 G. Nägele, *Physics Reports*, 1996, **272**, 215–372.
2 P. Pusey, H. Fijnaut and A. Vrij, *The Journal of Chemical Physics*, 1982, **77**, 4270–4281.
3 N. Boon, G. I. Guerrero-García, R. Van Roij and M. Olvera de la Cruz, *Proceedings of the National Academy of Sciences*, 2015, **112**, 9242–9246.
4 A. Torres, G. Téllez and R. van Roij, *The Journal of chemical physics*, 2008, **128**, 154906.
5 G. Bareigts and C. Labbez, *The Journal of Chemical Physics*, 2018, **149**, 244903.
6 J. Phalakornkul, A. Gast, R. Pecora, G. Nägele, A. Ferrante, B. Mandl-Steininger and R. Klein, *Physical Review E*, 1996, **54**, 661.
7 F. J. Rogers and D. A. Young, *Physical Review A*, 1984, **30**, 999.
8 M. Heinen, P. Holmqvist, A. J. Banchio and G. Nägele, *The Journal of chemical physics*, 2011, **134**, 044532.
9 J. Gapinski, G. Nägele and A. Patkowski, *The Journal of Chemical Physics*, 2012, **136**, 024507.
10 Y. Hallez and M. Meireles, *Langmuir*, 2017, **33**, 10051–10060.
11 Y. Hallez and M. Meireles, *The European Physical Journal E*, 2018, **41**, 1–5.

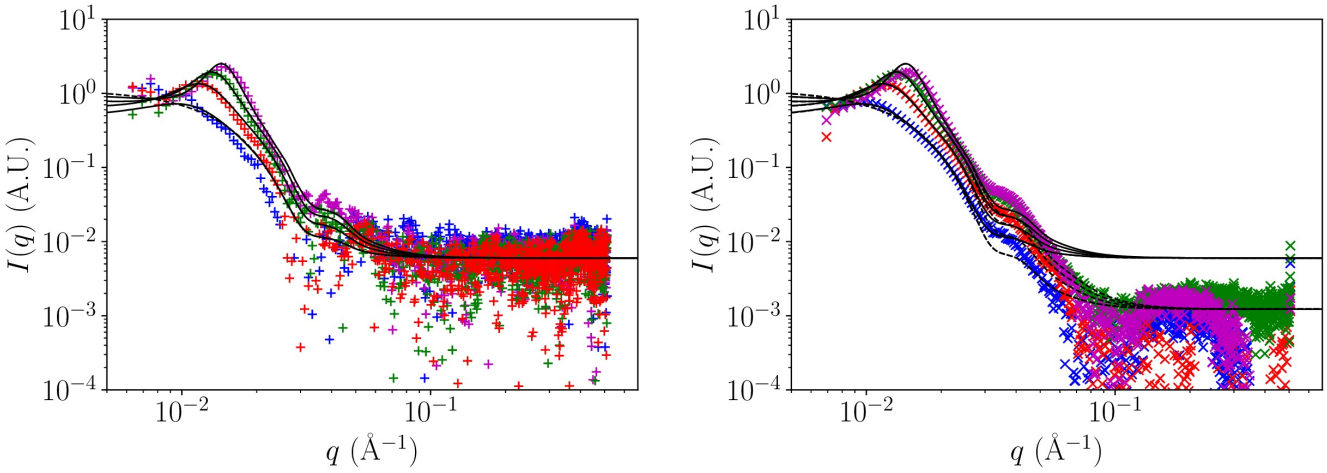

Fig. 1 SAXS signal from latex dispersions measured in the microfluidic chip (left) and in quartz capillaries (right). The left figure is the same as Fig. 6 in the main text but with a wider intensity range. Models fitted in the left figure are reproduced in the right figure as continuous lines to ease comparison. The same models but with a lower background are also reported with dashed lines.